https://doi.org/10.5194/egusphere-2025-4186
Preprint. Discussion started: 11 September 2025

Anomalous fading correction in luminescence dating – a mathematical reappraisal

Benny Guralnik[1*], Georgina E. King[1]

[1] Institute of Earth Surface Dynamics, University of Lausanne, Lausanne, 1015, Switzerland
[*] Present address: KLA Corporation, Diplomvej 373, Kgs Lyngby DK-2800, Denmark

Correspondence: benny.guralnik@gmail.com, georgina.king@unil.com

Abstract

Anomalous fading is a power law decay of trapped charge over time that is commonly observed in wide-bandgap semiconductors, leading to age underestimation in luminescence dating if unaccounted for. In this paper, we reappraise the mathematical foundations of luminescence signal correction and introduce two new closed-form analytical expressions for the two most commonly used age correction models, namely that of Huntley and Lamothe [*Can. J. Earth Sci. 38, 1093-1106, 2001*], and of Kars et al. [*Radiat. Meas., 43, 786-790, 2008*]. These expressions are amenable to straightforward uncertainty propagation, matching results from Monte-Carlo simulations at a fraction of the calculation cost. Additionally, we explore unorthodox combinations of signal fading and growth pathways, by coupling fading models to signal growth obeying general order kinetics, as well as the one-trap one-recombination center model.

1. Introduction

Anomalous fading is, to date, an undisputedly convoluted subdiscipline in luminescence dating that creates equal discomfort for students and professors alike. As a result, the community resorts to "black-box" solutions that include recirculation of measurement protocols, spreadsheets, and data analysis packages, all of which avoid reappraising the (often insecure) mathematical footing of the various correction approaches. Deviation from this "grey literature" can be challenging to justify, thereby stalling further progress. While we acknowledge the fundamental value of the various contributions on fading quantification and correction, the gaps in the mathematical clarity and self-consistency of the seminal papers in the field are nevertheless deep and chronic, and must be addressed transparently to allow meaningful progress going forward. The errors in prior studies generally fall into one of the following categories:

1) Mathematically erroneous statements: Wintle's (1973) seminal paper made an erroneous and misleading assertion with respect to its very central finding (Fig. 1a) by claiming that "*the shape of the decay curve does not, however, conform to any simple time dependence*", despite the fact that a simple time dependence (inset in Fig. 1a) was already well established in that context (cf. Hoogenstraaten, 1958; Thomas et al., 1965). Similarly, Huntley and Lamothe (2001) put forth a demonstrably incorrect claim that their fading correction scheme is "*restricted to the low-dose, linear portion of the dose response*" (see Section 5) – which nevertheless became a legitimate excuse for when corrected ages fall short of their independent constraints.

https://doi.org/10.5194/egusphere-2025-4186
Preprint. Discussion started: 11 September 2025

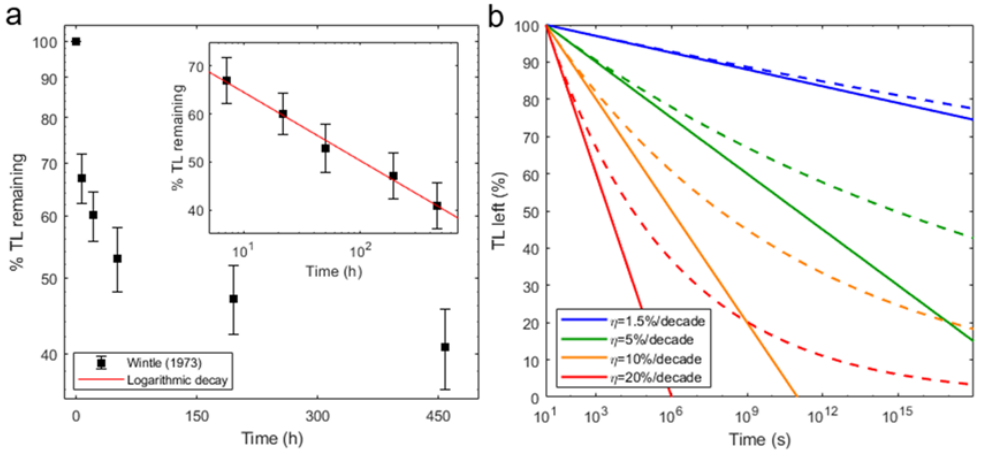

Figure 1. Characteristic problems with anomalous fading literature. a) Erroneous statements: "the shape of the decay curve does not […] conform to any simple time dependence" (Wintle, 1973); inset: same data on a linear signal time vs. logarithmic time axes, exhibiting a simple logarithmic decay at a ~29% fading rate (reference time of 2 days). b) Erroneous derivation: negative concentrations in the model of Visocekas (1985) are inevitable (continuous lines), but can be easily mitigated via a more informed integration (dashed lines, see text). c) Missing formulas from the literature: three examples of seminal formulas, whose building blocks are scattered across their corresponding papers but never brought together in a meaningful manner. The parameters are $\dot{D}$ for dose rate (with subscripts "*nat*" and "*lab*" corresponding to natural and laboratory, respectively), D_e and D_0 for equivalent and characteristic dose (respectively), t for time and T_{corr} for corrected age, n for the trapped electrons concentration evolving from initial n_0 to saturation N, g for the fading rate (g-value, unitless) for a reference time t_c, ρ' for rescaled g-value assuming escape frequency s, r' a dimensionless electron-hole separation distance.

2) Inadequate derivations: Visocekas (1976) made the first quantitative reinterpretation of Wintle's (1973) data (inset in Fig. 1a), however, his definition of the logarithmic decay constant (Visocekas, 1985) is at odds with his subsequent derivation, reflecting a faulty integration that not only led to wrong units but also invoked an unphysical model (continuous lines in Fig. 1b). As we show in Section 2, a self-consistent integration instantaneously leads to more meaningful results (dashed lines in Fig. 1b; see Section 3), precluding negative concentrations and foreshadowing the model of Huntley (2006). Similarly, the "-1" term in Eq. A4 of Huntley and Lamothe (2001) does not follow from $T_L \ll T$ as claimed but rather stems from a totally different assumption of $T_L = t_c$, the relaxation of which could lead to any other arbitrary "$-T_L/t_c$" offset in their age correction formula.

3) Misleading equations: The age correction formula of Huntley and Lamothe (2001, Eq. [A5]) lacks a key step, namely the rescaling of κ, which the authors do describe in the text

https://doi.org/10.5194/egusphere-2025-4186
Preprint. Discussion started: 11 September 2025

but omit from their arithmetic. As trivial as it may be, the rescaling of a g-value from one reference time t_1 to another t_2, via $g_2 = [g_1^{-1} - \log_{10}(t_2/t_1)]^{-1}$ is not reported in Huntley and Lamothe (2001) or any later publication. Our confidence in restating their formula arises from our successful reverse-engineering of their numerical examples. A similar failure to mathematically express the paper's central result repeats itself in Huntley (2006) which failed to formally define r'_{eff} (Fig. 1c) prior to its approximation. Furthermore, Kars et al. (2008) only provided a bare rate equation, leaving the reader to imagine how to combine it with the spatial distribution of electron-hole separation distances, even though a semi-analytical solution is straightforward (Fig. 1c).

The compound effect of these mathematical shortcomings, only partially listed above and illustrated in Fig. 1, has been chronic and additive: 1) erroneous statements curb the practitioners' understanding and stall further progress, sometimes for decades; 2) the few and far between mathematical derivations are taken as unquestionable truths rather than as steps towards better formulations; 3) the theoretical gaps lead to the proliferation of "grey" literature, spreadsheets and software, and of divergent practical implementations, each patching the shortcomings to the best of its authors' understanding, while still all referring to the method as one and the same. Our current contribution is written out of deep respect for all the fields' trailblazers, but recognises the need for mathematical clarity for the treatment of fading quantification and correction. We therefore proceed to give the shortest possible mathematical reappraisal of anomalous fading, followed by its verification, and finally some unforeseen and unprecedented variations on this rather old theme.

2. Exponential, logarithmic, and power-law decay

To define radioactive decay, Rutherford (1900) designated λ as the proportionality constant between concentration n and its decay rate with time dn/dt. Rearranging for λ and keeping its sign convention, we can express the decay constant as:

$$\lambda = -\frac{dn/n}{dt}. \tag{1}$$

where the right-hand side corresponds to fractional loss of concentration ($-dn/n$) per unit time (dt). Separation of variables and integration leads to the familiar $n(t)/n_0 = \exp(-\lambda t)$, in which $t = \lambda^{-1}$ is the amount of time it takes concentration to e-fold (i.e. reduce to $1/e$ of its initial value at $t = 0$).

Visocekas (1976, 1985) both coined the term "logarithmic decay", and defined the associated decay constant as "the slope of the TL light sum vs. ln t", which following our nomenclature of n for concentration (=the light sum in TL), and utilizing the identity $d(\ln t) = dt/t$, can be formally written as:

$$\eta = -\frac{dn}{dt/t}. \tag{2}$$

which should have had units of concentration. However, a few lines following his definition, Visocekas (1985) arbitrarily rescaled the denominator from $d\ln t$ to $d\log_{10} t$ (invoking the familiar "per decade of time"), and further assigned units of [%] to η's numerator, thus disclosing a miscommunicated normalization of η by some arbitrary concentration n_c. It is the proliferation of these faux units in the literature ("% per decade"), and their hardcoding into all subsequent formulas (cf. Visocekas, 1985; Huntley and Lamothe, 2001; cf. Slater et al., 2001), that leaves little doubt that Visocekas' "logarithmic decay" (Eq. 2) was in fact a misnomer, and that the proper naming should have invoked the concept of a power-law decay:

https://doi.org/10.5194/egusphere-2025-4186
Preprint. Discussion started: 11 September 2025

$$\kappa = -\frac{dn/n}{dt/t}. \quad (3)$$

where fractional concentration loss $-dn/n$ is scaled by fractional (rather than absolute, cf. Eq. 1) progression in time dt/t. Note that our new expression for κ (sensu Huntley and Lamothe, 2001) is a classic example of "dimensionless sensitivity" (Beck, 1970; Smith, 1994; Smertenko, 2020), defined as the "*fractional change in [a] calculated observable divided by the corresponding fractional change in the [corresponding] parameter of the model*" (Smith, 1994). Below we show that it is specifically Eq. (3), that all familiar results can be easily derived from. Visocekas' (1985) own seminal decay formula (straight lines in Figs. 1a-b):

$$\frac{n(t)}{n_c} = 1 - \kappa \ln\left(\frac{t}{t_c}\right) \quad (4)$$

may be understood as integration of Eq. (3) subject to a fixed scaling concentration, namely $\int dn/n_c = -\int \kappa\, dt/t$ (cf. Eq. 2) with $n_c = n(t_c) = const$ as the boundary condition. Serving as the starting point for the age correction of Huntley and Lamothe (2001), Eq. (4) is however unphysical, since n must inevitably, sooner or later, plunge into negative concentrations. This "feature" of the model bothered Visocekas (1985; one must drop the second term of his Eq. 7 to reproduce F in his Fig. 3). However, the negative concentrations can be overcome by integrating Eq. (3) as written, with no fixed scaling, to obtain:

$$\frac{n(t)}{n_c} = \exp\left[-\kappa \ln\left(\frac{t}{t_c}\right)\right] \quad (5)$$

Eq. (5) is the physical model that Visocekas probably strived for, where concentration remains positive $n > 0$ at all times (for a demonstration of its successful application, see Section 4). Note that the more familiar Eq. (4) may be considered as a special case of Eq. (5) in its linear region, where $\exp(-x) \approx 1 - x$. For typical laboratory conditions, the curvature of Eq. (5) is unnoticeable: consider the dashed green curve in Fig. 1b (g=5%), which could easily be mistaken for a logarithmic decay (Eq. 2) over 6-7 orders of magnitude of time. Let us reiterate, that κ in Eqs. (3-5) is just a unitless number, whose arbitrary rescaling and association with faux units ("% per decade") might have resulted in more confusion than enlightenment.

If κ (or the more commonly used g-value, defined as $g = \kappa \ln 10$) is obtained by fitting Eq. (4), one must report the vicinity of t around which it has been derived. This is known as the "reference time" t_c, which is conventionally set to 2 days (reflecting the typical timescale of a laboratory experiment). Although few laboratories take the trouble to report their t_c duration, and even fewer provide its units (i.e. is it 2 days but in units of [ka]?), t_c is a crucial parameter for validating one's data analysis. Due to the logarithm in the denominator of Eq. (4), the decay constant (whether κ or g) is only weakly dependent on the choice of the reference time t_c (see Eq. 6 below). Rescaling from one t_c to another is trivial. Consider a first triplet (κ_1, t_1, n_1) consisting of a decay constant κ_1, defined at the reference time t_1 and corresponding to concentration n_1. Consider a second triplet (κ_2, t_2, n_2) obeying the very same definition. Cross-referencing the concentrations via two instances of Eq. (4):

$$\frac{n_2}{n_1} = 1 - \kappa_1 \ln\left(\frac{t_2}{t_1}\right), \qquad \frac{n_1}{n_2} = 1 - \kappa_2 \ln\left(\frac{t_1}{t_2}\right).$$

we notice that the product of these two expressions cancels the concentrations, leaving us with $[1 - \kappa_1 \ln(t_2/t_1)][1 - \kappa_2 \ln(t_1/t_2)] = 1$, which after rearrangement and isolation of κ_2 yields:

$$\kappa_2 = \left[\kappa_1^{-1} - \ln\left(\frac{t_2}{t_1}\right)\right]^{-1}, \qquad g_2 = \left[g_1^{-1} - \log_{10}\left(\frac{t_2}{t_1}\right)\right]^{-1}. \quad (6)$$

Conceptually we notice that for $t_2 = t_1$, no rescaling should occur as expected. To verify the validity of Eq. (6), we successfully apply it to rescale $g_1 = 5\%$ from $t_1 = 2$ days to $\kappa_2 =$

https://doi.org/10.5194/egusphere-2025-4186
Preprint. Discussion started: 11 September 2025

0.0231 at $t_2 = 30$ (Appendix A of Huntley and Lamothe, 2001). It is easy to show that with a factor 15 increase of the reference time, the rescaled $g_2 = 1/(20 - 1.17) = 5.31\%$ is only marginally shifted by factor 1.06 from its initial value (as a rule of thumb, an order of magnitude change in time exerts a g-value change in the g-value itself). Note that the above rescaling applies for logarithmic decay only (Eq. 4), since for decay obeying true power-law (Eq. 5), κ remains constant over the entire range of times – which finally brings us to the nearest-neighbour distribution model as discussed next.

A physical model approximating power-law decay, which we will henceforth refer to as nearest-neighbor distribution (NND) trap decay, entered mainstream luminescence dating due to the combined efforts of Huntley (2006), who popularized rather ancient results in an accessible manner, and Kars et al. (2008) who coupled Huntley's catchy formulation to a realistic trap repopulation model. The NND trap decay model, nowadays most often ascribed to Tachiya and Mozumder (1974), in fact stems from Hoogenstraaten's (1958) theory of centres. In fact, Hoogenstraaten's numerically-exhaustive Eqs. (12.18a-b) immediately lead to Huntley's (2006) formulation under the approximations $t \cong \theta z$ and $f \cong \ln^3 z$ (which Hoogenstraaten must himself have resorted to for the calculation of his Fig. 8; cf. Fig. 2 in Huntley, 2006). In a nutshell, the NND trap decay model assumes a distribution of electron-hole separation distances, where the probability of finding a nearest neighbor at r' is given by $p(r') = 3r'^2 \exp(-r'^3)$. The tunneling rate to a center at r' is $K(r') = s \exp\left(-\rho'^{-1/3} r'\right)$, in which s is the tunneling frequency (s^{-1}), and ρ' (dimensionless) the nearest-neighbour distribution density. NND trap decay presumes that trapped electrons are lost via electron tunneling to the nearest available recombination centres, that gradually become situated farther and farther away as each progressive spherical shell of available centres is consumed. To calculate the surviving trapped charge concentration, one integrates over the remaining recombination centre population over all distances, or alternatively only from the effective "shell" at radius r'_{eff} at which fading is maximal at time t:

$$\frac{n(t)}{n_0} = \int_0^{\infty} 3r'^2 \exp(-r'^3)\, e^{-s \exp\left(-\rho'^{-1/3} r'\right) t} dr' = \int_{r'_{\text{eff}}}^{\infty} 3r'^2 \exp(-r'^3)\, dr' \cong \exp[-\rho' \ln^3(1.8\, s\, t)]. \quad (7)$$

Note that the effective radius $r'_{\text{eff}} \cong \rho'^{1/3} \ln(1.8\, s\, t)$ is obtained by setting the time to the inverse of the decay constant $t = 1/K\left(r'_{eff}\right)$ and inverting for r'_{eff}; note that 1.8 is a totally arbitrary constant, that improved the approximation in the few scenarios considered by Huntley (2006). Note also that the resulting $n(t)/n_0 \cong \exp[-\rho' \ln^3(1.8\, s\, t)]$ is conspicuously similar to our Eq. (5), where the roles of ρ' and s are analogous to those of κ and t_c^{-1}, respectively. Yet unlike in the heuristic Eq. (5), the logarithm of time in Eq. (7) is cubed, disclosing the effect of volumetric integration (Hoogenstraaten, 1958; Tachiya and Mozumder, 1974). To show that ρ' is merely a rescaled g-value, we differentiate Eq. (7) with respect to time, scale by t/n (cf. Eq. 3), and rearrange to obtain:

$$\rho' = \frac{\log_{10} e}{3 \ln^2(1.8\, s\, t_c)} \cdot g. \quad (8)$$

Just like Eq. (6), Eq. (8) is also an extremely useful relationship that has so far not been spelled out in the literature.

3. Common age corrections

3.1 Huntley and Lamothe, 2001

The Huntley and Lamothe (2001) age correction is a direct utilization of Visocekas' logarithmic decay law (Eq. 4), hinted at a decade and a half earlier in Aitken (1985) yet never put into a practical mathematical formulation. Below, we break down the numerical example

https://doi.org/10.5194/egusphere-2025-4186
Preprint. Discussion started: 11 September 2025

from Appendix A of Huntley and Lamothe (2001) and use it to rewrite their formulas in a more meaningful manner.

a) First, one conducts laboratory fading experiments, and best fits them via Eq. (4) to obtain a decay constant κ referenced to a common t_c across all samples to allow for straightforward comparison ($\kappa = 5\%/\ln\ 10 = 0.0217$ for $t_c = 2$ days).
b) Next, one must use Eq. (6) to rescale κ from a common t_c to a sample-specific t_{lab} via $\kappa_{lab} = [\kappa^{-1} - \ln(t_{lab}/t_c)]^{-1}$. The laboratory time t_{lab} can be defined as time spent by the sample to attain its equivalent dose, D_e, in the laboratory; such a definition is broad enough to both contain the straightforward $t_{lab} = D_e/\dot{D}_{lab}$ in which $\dot{D}_{lab}$ is the laboratory dose rate, as well as an arbitrary prescribed amount of fading time to correct for (e.g. $t_{lab} = 30$ days from irradiation to measurement, leading to $\kappa_{lab} = 0.0231$; Huntley and Lamothe, 2001).
c) Finally, one uses Eq. (4) again to write $n(t)/n_0 = 1 - \kappa_{lab}\ln(t/t_{lab})$, and solves for the initial concentration to obtain $n_0 = n(t)/[1 - \kappa_{lab}\ln(t/t_{lab})]$. Granted linearity between concentration and apparent age, we replace $n(t)/n_0 = t_{faded}/t_{corr}$, obtaining:

$$t_{corr} = \frac{t_{faded}}{1 - \left[\kappa^{-1} - \ln\left(\frac{t_{lab}}{t_c}\right)\right]^{-1}\ln\left(\frac{t_{corr}}{t_{lab}} + C\right)}.$$

4) where C is a contested offset (Lamothe et al., 2003), set to $C = -1$ in Huntley and Lamothe (2001) even though their $T_L \ll T$ assumption should have led to $C = -T_L/t_c$ in the equation above. Note that in the equation above, t_{corr} may be obtained via fixed-point iteration. Given t_{faded} of 10^2, 10^3, and 10^4 years, and complying with $C = -1$, we set $t_{corr} = t_{faded}$ in the right hand side, recalculate t_{corr} on the left hand side, and repeat 2-3 iterations to converge to t_{corr} of 116.9, 1248.6, and 13402 years, in accordance with Huntley and Lamothe (2001).

Since long delayed-readout experiments (Auclair et al., 2003) have never entered the mainstream due to their impracticality, we feel entitled to substitute $t_{faded} = D_e/\dot{D}_{nat}$ in which $\dot{D}_{nat}$ is the natural dose rate, $t_{lab} = D_e/\dot{D}_{lab}$ as already mentioned before, and rewrite Huntley and Lamothe's (2001) age equation as:

$$t_{\mathrm{corr}} = \frac{D_e/\dot{D}_{nat}}{1 - \left[\kappa^{-1} - \ln\left(\frac{D_e/\dot{D}_{lab}}{t_c}\right)\right]^{-1}\ln\left(\frac{t_{\mathrm{corr}}}{D_e/\dot{D}_{lab}} - 1\right)}. \quad (9)$$

keeping the familiar "-1" offset for historical rather than mathematical reasons. Noticing that a dual occurrence of an unknown (here t_{corr}) across both sides of an equation, one raw and one logarithmic, is the hallmark of problems amenable to a solution via Lambert's W function (Corless, 1996), we find that the implicit Eq. (9) has an exact, explicit solution that reads:

$$t_{\mathrm{corr}} = \frac{D_e/\dot{D}_{lab}}{\exp\left(W_{-1}\left\{-\frac{\dot{D}_{lab}}{\dot{D}_{nat}}\left(\left[1 + \frac{1}{\kappa} - \ln\left(\frac{D_e}{\dot{D}_{lab}t_c}\right)\right] - 1\right)e^{-\left[1+\frac{1}{\kappa}-\ln\left(\frac{D_e}{\dot{D}_{lab}t_c}\right)\right]}\right\} + \left[1 + \frac{1}{\kappa} - \ln\left(\frac{D_e}{\dot{D}_{lab}t_c}\right)\right]\right)}. \quad (10)$$

where $W_{-1}(x)$ is the -1 branch of Lambert's W function, and the term $\dot{D}_{lab}/\dot{D}_{nat}$ has been foreshadowed by Lamothe et al. (2003). Despite the lengthy expression, the derivation of Eq. (10) from Eq. (9) becomes trivial upon the following reparameterization:

$$t_{\mathrm{corr}} = \frac{D_e/\dot{D}_{nat}}{f}, f = \frac{\dot{D}_{lab}}{\dot{D}_{nat}}e^{-q-p}, p = 1 + \frac{1}{\kappa} - \ln\left(\frac{D_e}{\dot{D}_{lab}t_c}\right), q = W_{-1}\left[-\frac{\dot{D}_{lab}}{\dot{D}_{nat}}(p-1)e^{-p}\right].$$

https://doi.org/10.5194/egusphere-2025-4186
Preprint. Discussion started: 11 September 2025

where f is a fading correction factor, whose associated uncertainty with respect to κ can be obtained via the chain rule, namely $\frac{df}{dp} = f\left[1 - \frac{(p-2)q}{(p-1)(q+1)}\right]$, $\frac{dp}{d\kappa} = -\kappa^{-2}$, $\frac{df}{d\kappa} = \frac{df}{dp}\frac{dp}{d\kappa}$, to yield a fully analytical propagation of all uncertainties in Eq. (10) as follows:

$$\sigma t_{\mathrm{corr}} = \sqrt{\left(\frac{\sigma D_e}{D_e}\right)^2 + \left(\frac{\sigma \dot{D}_{nat}}{\dot{D}_{nat}}\right)^2 + \left(\left[\frac{(p-2)q}{(p-1)(q+1)} - 1\right]\frac{\sigma_\kappa}{\kappa^2}\right)^2}. \quad (11)$$

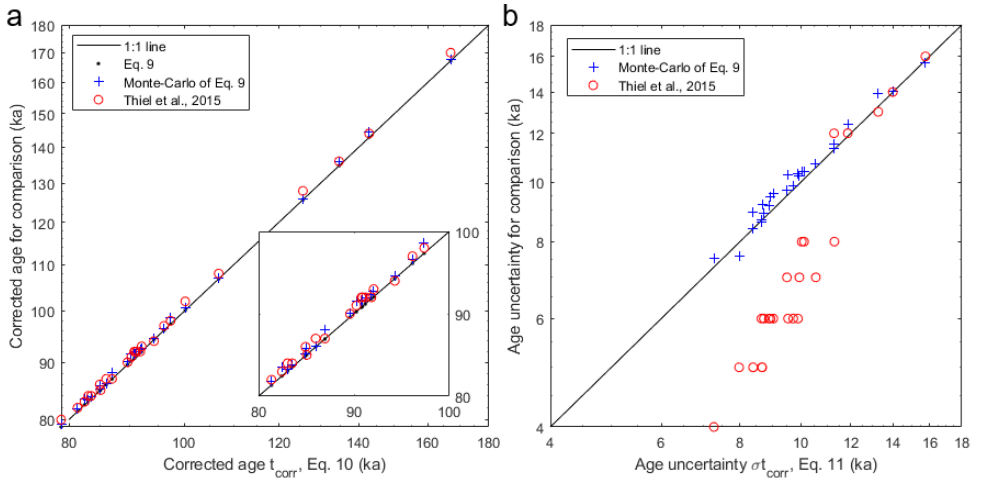

Figure 2. a) comparison of our new explicit Eqs. (10) and (11) to former approaches, as demonstrated on the data of Thiel et al., 2015. a) age from the explicit Eq. (10) vs. the implicit age from Eq. (9) both as a single-instance (black dots) and averaged Monte-Carlo simulations (blue crosses), and published results (red circles). b) age uncertainty from the explicit Eq. (11) vs. standard deviation from Monte-Carlo simulations (blue crosses), and published results (red circles). See appendix B for tabulated values.

We test our new formulas on the extensive sedimentary archive of Thiel et al. (2015), consisting of 25 feldspar pIR-IR$_{225}$ ages from Oga peninsula (Japan), where D_e, g, and $\dot{D}_{nat}$ and their uncertainties have all been measured and reported (Appendix A). To evaluate $W_{-1}(x)$ in Eq. (10), we use the recent and high-precision algorithm of Lóczi (2022). Our Eqs. (9-10) yield identical results within 16-digit numerical precision (Fig. 2a), whose relative sub-percent deviation (-0.9% on average) from Thiel et al.'s ages is the direct result of the latter's reporting of ages in [ka] units with zero significant digits. The negligible deviation of Monte-Carlo age estimates (-0.66% on average) from the analytical equations confirms that the effects of measurement uncertainties (σD_e, σg, and $\sigma \dot{D}_{nat}$) propagate linearly into the age correction. Fig. 2b demonstrates that Eq. (11) matches Monte-Carlo estimates of age uncertainties across almost an octave of σt_{corr} within high accuracy (2.6% on average). Conversely, the age uncertainties reported by Thiel et al. (2015) (red circles Fig. 2b) are not only visibly rounded to the nearest integers, but they progressively underestimate (by up to a factor of 2) the actual age uncertainties with younger age. The latter artefact arises from the community's most popular fading-correction spreadsheet, which is almost never given credit to (see Jaiswal et al., 2009 for a refreshing exception). In that otherwise excellent spreadsheet, propagation of age uncertainties is done via a finite number of calculated end-member scenarios, which may be insufficient for younger ages vis-à-vis the analytical approach of Eq. 11.

3.2 Kars et al., 2008

https://doi.org/10.5194/egusphere-2025-4186
Preprint. Discussion started: 11 September 2025

Kars et al. (2008) coupled the model of Huntley (2006) to trap repopulation via the environmental dose rate $\dot{D}_{nat}$ under the effect of a saturating exponential growth, where the filling of a finite number of traps N is limited by the characteristic dose D_0, which can be thought of as the e-folding radiation dose absent any fading effects. Recasting Kars' model into a single semi-analytical equation, one obtains:

$$\frac{n(t)}{N} = \int_0^\infty \frac{3r'^2 \exp(-r'^3)}{1 + \frac{D_0}{\dot{D}} s \exp\left(-\rho'^{-1/3} r'\right)} \left\{1 - e^{-\left[\dot{D}/D_0 + s \exp\left(-\rho'^{-1/3} r'\right)\right] t}\right\} dr'. \tag{12}$$

If one wishes to be pedantic, the age correction due to Kars can be formally written as:

$$\begin{aligned} &\int_0^\infty \frac{3r'^2 \exp(-r'^3)}{1 + \frac{D_0}{\dot{D}_{lab}} s \exp\left(-\rho'^{-1/3} r'\right)} \left\{1 - e^{-\left[\dot{D}_{lab}/D_0 + s \exp\left(-\rho'^{-1/3} r'\right)\right] D_e/\dot{D}_{lab}}\right\} dr' \\ &\qquad = \int_0^\infty \frac{3r'^2 \exp(-r'^3)}{1 + \frac{D_0}{\dot{D}_{nat}} s \exp\left(-\rho'^{-1/3} r'\right)} \left\{1 - e^{-\left[\dot{D}_{nat}/D_0 + s \exp\left(-\rho'^{-1/3} r'\right)\right] t_{\mathrm{corr}}}\right\} dr' \end{aligned} \tag{13}$$

where on the left-hand side we have fading-affected signal growth in the laboratory, to be matched by the term on the right-hand side, where fading affected growth to the same level occurs at an environmental dose rate during an unknown duration t_{corr}. As we show below, Eqs. (12-13) lack an exact solution, but are amenable to approximation if we extend the concept of effective radius r'_{eff} as follows. A foreshadowing of our new approximation is to be found in King et al. (2016), who multiplied the laboratory dose response curve $\left(1 - e^{-\dot{D}_{lab} t / D_0}\right)$ by Eq. (7) to obtain:

$$\frac{n(t)}{N} = \left[1 - \exp\left(-\frac{\dot{D}t}{D_0}\right)\right] \int_{r'_{\mathrm{eff}}}^\infty 3r'^2 \exp(-r'^3)\, dr' \cong \left[1 - \exp\left(-\frac{\dot{D}t}{D_0}\right)\right] \exp[-\rho' \ln^3(1.8\, s\, t^*)] \tag{14}$$

where t^* was taken to be half the irradiation time (Aitken 1985, p.279-280). The approximation in Eq. (14) is typically satisfactory for $t < 10^4$ s, but at longer times often results in an unphysical artefact of signal decay (e.g. Supplementary Fig. S2B and S3B in King et al., 2016; Fig. 3B and 3E in Bouscary and King, 2024), arising from the last exponential term in Eq. (14), which at long enough times brings $n(t)/N$ to zero (no such term exists on the exact, left-hand side of Eq. 14). This artefact can be easily mitigated if we approximate $r'_{\mathrm{eff}} \cong \rho'^{1/3} \ln\left(1.8\, s\, \frac{D_0}{\dot{D}} \left[1 - \exp\left(-\frac{\dot{D}t}{D_0}\right)\right]\right)$, from which it follows that at short times, $r'_{\mathrm{eff}}(t \to 0) \cong \rho'^{1/3} \ln(1.8\, s\, t)$, reducing r'_{eff} to Huntley's formulation (2006), while at long times, $r'_{\mathrm{eff}}(t \to \infty) \cong \rho'^{1/3} \ln\left(1.8\, s\, D_0/\dot{D}\right)$, representing a "frozen" fading front counteracted by trap refilling at a commensurate rate. Substituting our alternative definition of r'_{eff} into Eq. (13) we get:

$$\frac{n(t)}{N} \cong \left[1 - \exp\left(-\frac{\dot{D}t}{D_0}\right)\right] \exp\left(-\rho' \ln^3 \left\{1.8\, s \frac{D_0}{\dot{D}} \left[1 - \exp\left(-\frac{\dot{D}t}{D_0}\right)\right]\right\}\right). \tag{15}$$

which for typical parameters matches numerical integration of Eq. (12) to within sub-percent accuracy. By equating two instances of Eq. (15), one for natural $\dot{D} = \dot{D}_{\mathrm{nat}}$, and the other for laboratory $\dot{D} = \dot{D}_{\mathrm{lab}}$ growth (cf. Eq. 13), we obtain:

https://doi.org/10.5194/egusphere-2025-4186
Preprint. Discussion started: 11 September 2025

$$t_{corr} = -\frac{D_0}{\dot{D}_{\mathrm{nat}}}\ln\left\{1-\left(1-e^{-\frac{D_e}{D_0}}\right)\frac{\exp\left[-\rho'\ln^3\left(1.8\,s\,\frac{D_0}{\dot{D}_{\mathrm{lab}}}\left(1-e^{-\frac{D_e}{D_0}}\right)\right)\right]}{\exp\left[-\rho'\ln^3\left(1.8\,s\,\frac{D_0}{\dot{D}_{\mathrm{nat}}}\left(1-e^{-\frac{D_e}{D_0}}\right)\right)\right]}\right\}. \quad (16)$$

As with Eq. (10), we rewrite Eq. (16) more compactly, which allows us to derive its analytical uncertainty propagation more easily:

$$t_{corr} = -\frac{D_0}{\dot{D}_{\mathrm{nat}}}\ln(1-rn_e), r = e^{-\rho'\left[\ln^3\left(1.8\,s\frac{D_0}{\dot{D}_{\mathrm{lab}}}n_e\right)-\ln^3\left(1.8\,s\frac{D_0}{\dot{D}_{\mathrm{nat}}}n_e\right)\right]}, n_e = \left(1-e^{-\frac{D_e}{D_0}}\right).$$

$$\frac{dt_{corr}}{d\rho'} = \frac{-D_0 n_e r}{\dot{D}_{\mathrm{nat}}(1-n_e r)}\left[\ln^3\left(1.8\,s\,\frac{D_0}{\dot{D}_{\mathrm{lab}}}\,n_e\right)-\ln^3\left(1.8\,s\,\frac{D_0}{\dot{D}_{\mathrm{nat}}}\,n_e\right)\right].$$

$$\frac{dt_{corr}}{dD_0} = -\frac{\ln(1-n_e r)}{\dot{D}_{\mathrm{nat}}} - \frac{D_e(1-n_e)r}{D_0\dot{D}_{\mathrm{nat}}(1-n_e r)} - 3\,\rho' r\frac{n_e - D_e(1-n_e)}{D_0\dot{D}_{\mathrm{nat}}(1-n_e r)}\left[\ln^2\left(1.8\,s\,\frac{D_0}{\dot{D}_{\mathrm{lab}}}\,n_e\right)-\ln^2\left(1.8\,s\,\frac{D_0}{\dot{D}_{\mathrm{nat}}}\,n_e\right)\right].$$

$$\sigma t_{corr} = \sqrt{t_{corr}^2\left[\left(\frac{\sigma D_e}{D_e}\right)^2+\left(\frac{\sigma\dot{D}_{nat}}{\dot{D}_{nat}}\right)^2\right]+\left(\frac{dt_{corr}}{d\rho'}\cdot\sigma\rho'\right)^2+\left(\frac{dt_{corr}}{dD_0}\cdot\sigma D_0\right)^2}. \quad (17)$$

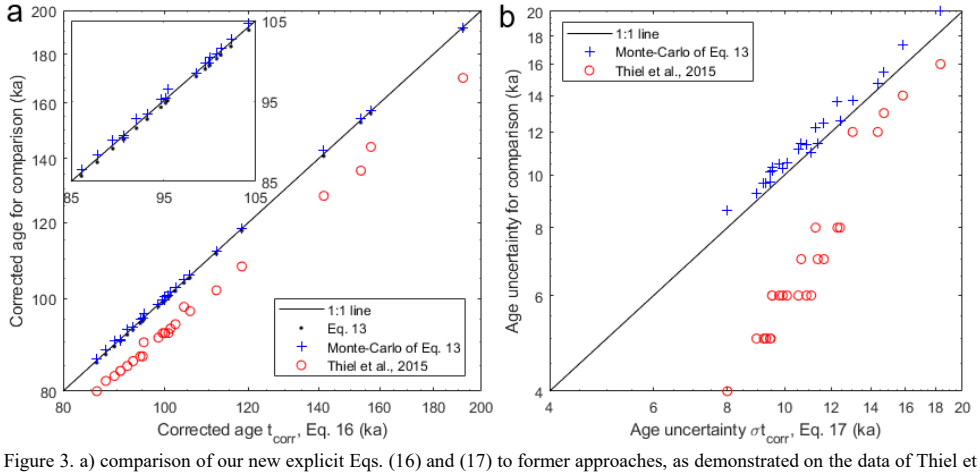

Figure 3. a) comparison of our new explicit Eqs. (16) and (17) to former approaches, as demonstrated on the data of Thiel et al., 2015. a) age from the explicit Eq. (16) vs. the implicit age from Eq. (13) both as a single-instance (black dots) and averaged Monte-Carlo simulations (blue crosses), and published results (red circles). b) age uncertainty from the explicit Eq. (17) vs. standard deviation from Monte-Carlo simulations (blue crosses), and published results (red circles). See appendix B for tabulated values.

We test our new formulas on the same dataset as before, using an "unfaded" estimate of D_0 =476 Gy (cf. Fig 5b in Section 4 below). The relative accuracy of the Kars model approximation (Eq. 16) vis-à-vis the exact numerical quadrature of the Kars et al. (2008) model (Eq. 13) is 0.5%. As in Fig. 2, only a negligible deviation of Monte-Carlo age estimates (-0.79% on average) from the analytical equations is detectable. A systematic model-to-model offset, whereby the Kars et al. (2008) yields 9.3±1.9% older ages than the Huntley and Lamothe (2001), is apparent. For discussion on age accuracy vis-à-vis independent constraints ("which

https://doi.org/10.5194/egusphere-2025-4186
Preprint. Discussion started: 11 September 2025

model is right?"), we refer the reader to Section 4.4. Furthermore, Fig. 3b demonstrates that σt_{corr} values obtained using Eq. (17) underestimate Monte-Carlo estimates by 5.0±2.8%, which we still consider as an excellent achievement, given that until now, there existed no alternatives to Monte-Carlo simulations for the estimation of the age uncertainties of the Kars et al. (2008) age correction.

4. Unorthodox age corrections

By disentangling the fundamental concepts related to quantification of fading rates (Section 2) and their derivative age corrections (Section 3), we recognize two straightforward model combinations that for some reason have never been put together before.

4.1. Age correction from NND decay

The following correction is similar to that of Huntley & Lamothe (2001) in that it uses the quantified fading rate to roll the time back to estimate n_0, yet instead of using logarithmic decay, the apparent faded age $D_e/\dot{D}_{nat}$ is divided by Eq. (7):

$$t_{corr} = \frac{D_e/\dot{D}_{nat}}{\exp[-\rho' \ln^3(1.8\, s\, t_{corr})]}. \tag{18}$$

Eq. (18) is analogous to Eq. (9), without rescaling of the g-value (since ρ' is a global parameter). Like Eq. (9), Eq. (18) too is implicit with respect to t_{corr}, but converges quickly via fixed-point iteration (i.e. an iterative procedure, where the left-hand side is updated by substituting its previous value into the right-hand side; initial guess for t_{corr} is $D_e/\dot{D}_{nat}$).

4.2. Saturating exponential signal growth, coupled to power law decay

The following correction is similar to that of Kars et al. (2008) in that it combines both signal growth and decay, yet instead of using a distribution of traps in combination with the NND model, here charge accumulates in a single trap (first term in parentheses), and decays from it following power law (Eq. 5):

$$\frac{n(t)}{N} = \left(1 - e^{-\frac{\dot{D}}{D_0}t}\right) \exp\left[-\kappa \ln\left(\frac{t}{t_c}\right)\right]. \tag{19}$$

Note the conceptual similarity of Eq. (19) with Eq. (15). To use Eq. (19) to correct an age, one equates between the signal obtained in the laboratory (left hand side below) and in nature (left hand side below), and solves for t_{corr}:

$$\left(1 - e^{-\frac{D_e}{D_0}}\right) \exp\left[-\kappa \ln\left(\frac{D_e/\dot{D}_{lab}}{t_c}\right)\right] = \left(1 - e^{-\frac{\dot{D}_{nat}}{D_0}t_{corr}}\right) \exp\left[-\kappa \ln\left(\frac{t_{corr}}{t_c}\right)\right].$$

4.3. Non-first order signal growth, coupled to NND decay

Starting with the model of Kars et al. (2008), we can replace their first-order rate equation to the one-trap one-recombination center (OTOR) model (Pagonis et al., 2020), yielding:

$$\frac{n(t)}{N} = \int_0^\infty 3r'^2 \exp(-r'^3)\, \hat{n}_{r'} dr', \qquad \frac{d\hat{n}_{r'}}{dt} = \frac{\dot{D}}{D_0} \cdot \frac{(1-\hat{n}_{r'})}{R + (1-\hat{n}_{r'})(1-R)} - s \exp\left(-\rho'^{-1/3} r'\right) \hat{n}_{r'} \tag{20}$$

where R is a dimensionless retrapping ratio (Pagonis et al., 2020). Note that since a special case of Eq. (20) with $R = 1$ amounts to the Kars et al. (2008) correction (cf. Eq. 12), Eq. (20) can be considered as a direct extension of the Kars et al. (2008) age correction scheme for cases where signal growth complies with the OTOR model. As a counterpart for Eq. (20), and purely for completeness (rather than novelty), we note an earlier and similar attempt at replacing first-order behavior with the general order kinetics (GOK) model (cf. Guralnik et al., 2015):

https://doi.org/10.5194/egusphere-2025-4186
Preprint. Discussion started: 11 September 2025

$$\frac{n(t)}{N} = \int_0^\infty 3r'^2 \exp(-r'^3)\, \hat{n}_{r'} dr', \qquad \frac{d\hat{n}_{r'}}{dt} = \frac{\dot{D}}{D_0}(1-\hat{n}_{r'})^\alpha - s\exp\left(-\rho'^{-1/3} r'\right)\hat{n}_{r'} \tag{21}$$

which conveniently reduces to the Kars et al. (2008) scheme given $\alpha = 1$. Note that while Eq. (21) has been successfully used in luminescence thermochronology (cf. Section 5), we are unaware of its applications for age correction in a sedimentary dating context. To use Eqs. 20 or 21 to correct an age, one equates two instances of the relevant equation (cf. Section 4.2), one expressing laboratory growth and the other growth in nature for an unknown duration t_{corr}, that one then solves for.

4.4. Benchmarking unorthodox vs. common age corrections vis-à-vis an independent age

The stratigraphic section studied by Thiel et al. (2015) contains two independently dated tephra markers which are widespread in northern Japan, namely the Toya ash (dated by various U-Pb and U-Th methods to ~0.1 Ma with a ~10% relative uncertainty; see Ito, 2024, and references therein) and the Aso-4 tephra (whose radiometric K-Ar age is 89±7 ka; Matsumoto, 1990). The only sample in Thiel et al. (2015) with sufficiently documented raw luminescence data to enable full age recalculation using all the approaches presented in this paper, is sample 055231, directly capped by the Toya ash. The horizontal line in Fig. 4c is a Toya tephra age of 112–115 ka as assigned by Thiel et al. (2015), from the references that were available to these authors at the time of writing. While model fits to the anomalous decay data (circles in Fig. 4a) and dose response (circles in Fig. 4b) are barely distinguishable, there is a considerable variance in the resulting pIR225 ages (circles with error bars in Fig. 4c), spanning 75–130 ka within 1σ uncertainties.

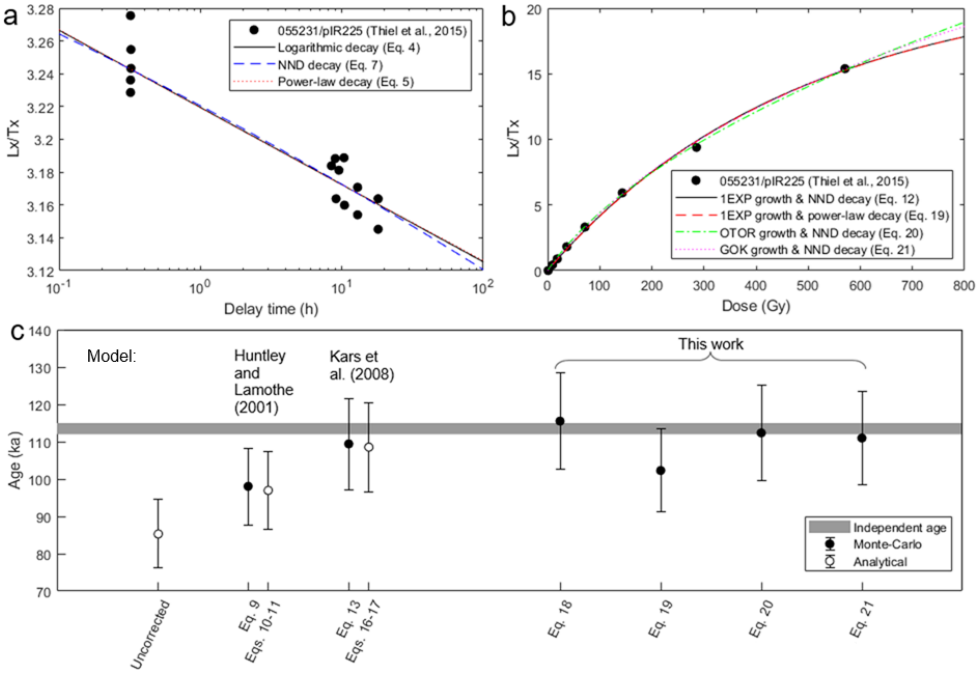

Figure 4. a) laboratory decay and b) dose response curve of pIR225 signal of sample 055231 from Thiel et al. (2015). c) luminescence ages following corrections considered in this study. The horizontal line corresponds to the independent age of 112-115 ka associated with the Toya tephra (Thiel et al., 2015 and references therein).

https://doi.org/10.5194/egusphere-2025-4186
Preprint. Discussion started: 11 September 2025

Within the methodological uncertainties of luminescence dating, the independent 112–115 ka age is matched by any of the *physical* corrections of IRSL fading (i.e. all except Huntley and Lamothe, 2001, which is based on the problematic logarithmic signal loss – see Section 2.) Note, that the fading corrected ages cluster into two groups, corresponding to the younger ages from non-NND models (Eqs. 9-11 and 19), in contrast to the older ages from the NND decay models (Eqs, 18, 20 and 21); the latter appear to yield results closer to the independent age constraint that Thiel et al. (2015) quoted. It is cautiously remarked that replacing the first-order signal growth of Kars et al. (2008) with either GOK or OTOR (Eqs. 20-21) seems to further increase model accuracy vis-à-vis the 112–115 ka age reference.

Regrettably, the exercise in Fig. 4c is too limited to draw any substantial conclusions regarding the validity of the anomalous fading corrections being tested, or lack thereof. Even for the reanalyzed sample (055231), Thiel et al.'s 112–115 ka age bracket is unrealistically narrow in light of the latest and most rigorous geochronological investigation of the Toya ash (Ito, 2024), which cautiously refers to that volcanic event as a ~0.1 Ma eruption with a 1σ age uncertainty of ~10% (cf. a U-Th isochron age of 110±14 ka, and weighted mean U-Pb age of 103±14 ka). With this latter and more realistic age constraint, any of the fading-corrected luminescence ages in Fig. 4c are in accord with the best available independent chronology (Ito, 2024).

While we lack dose response data for samples 055255 and 055256 to be able to conduct a similar exercise to that presented in Fig. 4, their results are also of interest and are discussed below. These samples, which bracket the 89±7 ka Aso-4 tephra from just below and above, yield weighted luminescence mean ages of 91.5±10.6 ka using the Huntley and Lamothe (2001) correction, and 99.7±11.6 ka using the Kars et al. (2008) model (Appendix B). Just as with the Toya ash, the independent age constraint doesn't allow discerning "which fading model is right": within methodological uncertainties, they all are. To explicitly warn the reader against confirmation bias that the Huntley and Lamothe (2001) correction (91.5±10.6 ka) falls "closer" to the K-Ar age, a few caveats regarding age accuracy are given. A potential for a <5% systematic age underestimation of the K-Ar system relative to its more accurate ^{40}Ar-^{39}Ar successor (Renne, 2006), could easily raise the independent age of the Aso-4 ash to 93.5±7 ka. An analogous but significantly larger systematic overestimation of <20%, affecting the luminescence chronometry, is potentially due to severe uncertainties with respect to dose rate $\dot{D}$ (cf. last two columns in Table 1 of Thiel et al., 2015, with Fig. S5 and Table S5 in Guralnik et al., 2015). In fact, Thiel et al. (2015) explicitly concluded their paper emphasising "the importance of investigating the mineral composition in more detail in order to get better dose rate estimates", and it is beyond all doubt that their mineralogical study (their Section 3.2 and Fig. 4) arose from an incipient mismatch of their feldspar IRSL ages with independent age control, when standard dose rate calculations led to severe (~20%) age underestimation vis-à-vis tephrochronology. Increasing all dose rates in Appendix A by even 10%, the fading-corrected pIR225 ages based on the Huntley and Lamothe (2001) and Kars et al. (2008) corrections would be ~82 ka and ~89 ka, respectively, with an opposite implication to that from before, i.e. that it is namely the Kars et al. (2008) model, which yields results which are "closer" to the independent K-Ar age.

The analysis above, and the naiveté of some of the straw arguments presented (which model is "closer" to independent age control), demonstrates that the distinction between different luminescence fading models, even in a "perfect" sedimentary archive with an abundance of solid external chronological constraints, can very quickly run into circular arguments at best. Extreme caution is therefore needed when reconciling between different chronologies (e.g. Guralnik et al., 2011), let alone promoting or dismissing models of one

https://doi.org/10.5194/egusphere-2025-4186
Preprint. Discussion started: 11 September 2025

method against results from another – which we simply dare not partake in. In light of the above, we find it necessary to end Section 4.4 with a disclaimer, that the aim of the present work has been solely to state all the luminescence fading models in a mathematically literate manner, and present correct and transparent calculations; it is entirely the practitioner's task to use these models responsibly, or as George Box once wittingly remarked, "all models are wrong, but some are useful".

5. Equilibrium ages

Robust independent age controls for sedimentary deposits are often difficult to establish, because of limited materials available for alternative dating methods, as well as the limitations of those methods themselves (e.g. ~50 ka detection limit of ^{14}C, potential open-system behaviour of U/Th, etc.). In contrast, a thermochronological constraint may offer a simpler case study, for rocks that have experienced isothermal storage of the luminescence system at a temperature, T_{nat}, for a period greatly exceeding the response time of that system. Due to its tectonic quiescence during the Quaternary, the KTB borehole offers an ideal setting for validation of trapped charged thermochronometers (Guralnik et al., 2015, and references therein). Eq. (22) below is a crude approximation of combining athermal and thermal losses of a luminescence system to predict its age (cf. Guralnik and Sohbati, 2019):

$$t_{\mathrm{model}} = -\frac{D_0}{\dot{D}_{\mathrm{nat}}}\ln(1-f_x\theta),\theta = \frac{\left[1+\frac{s_{th}\exp\left(-E_{eff}/k_BT_{\mathrm{nat}}\right)}{D_0/\dot{D}_{\mathrm{nat}}}\right]^{-1}}{\left[1+\frac{s_{th}\exp\left(-E_{eff}/k_BT_{\mathrm{lab}}\right)}{D_0/\dot{D}_{\mathrm{lab}}}\right]^{-1}}. \quad (22)$$

Where t_{model} is the model age, f_x is the athermal equilibrium factor, extracted from either Eq. (10) or (16):

$$f_{H\&L} = \frac{\dot{D}_{lab}}{\dot{D}_{nat}}e^{-q-p}, p = 1+\frac{1}{\kappa}-\ln\left(\frac{D_e}{\dot{D}_{lab}t_c}\right), q = W_{-1}\left[-\frac{\dot{D}_{lab}}{\dot{D}_{nat}}(p-1)e^{-p}\right] \quad (23)$$

$$f_{Kars} = \frac{\exp\left[-\rho'\ln^3\left(zsD_0/\dot{D}_{\mathrm{nat}}\right)\right]}{\exp\left[-\rho'\ln^3\left(zsD_0/\dot{D}_{\mathrm{lab}}\right)\right]} \quad (24)$$

while θ is a conceptually identical expression to f_x, yet accounting for thermal equilibrium (cf. Guralnik and Sohbati, 2019).

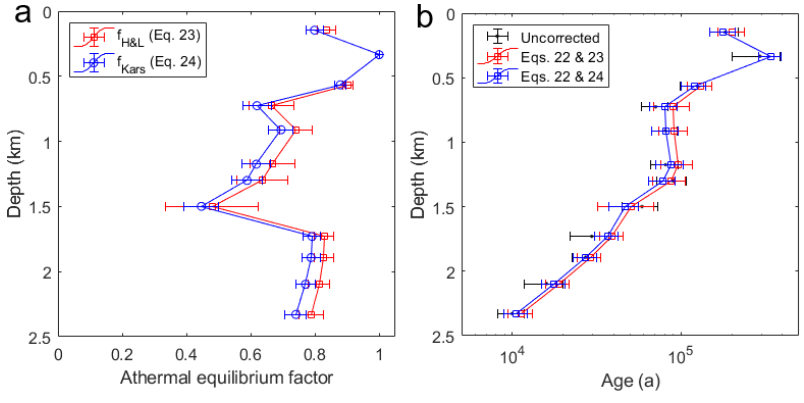

Figure 5: Equilibrium system at the KTB borehole, Germany. a) Athermal equilibrium factors from Eqs. (23-24), alongside thermal equilibrium (continuous curve), as a function of sample depth. b) observed vs. modelled ages vs. depth.

https://doi.org/10.5194/egusphere-2025-4186
Preprint. Discussion started: 11 September 2025

Fig. 5 demonstrates that Eq. (22) can be successfully used to quantitatively predict the observed ages of samples from the KTB borehole (Guralnik et al., 2015) across a broad range of g_{2d}=0 – 7 %/decade, and ~1.5 orders of magnitudes of apparent age (Appendix C). Note, that in Fig. 5b, the underground and laboratory temperatures obey $T_{nat}(z) = 7.5 + 27.5\ z$ [°C] and T_{lab}=15 °C, respectively, while the thermal stability of the $IRSL_{50}$ system is approximated as (a) uniform throughout the borehole (cf. Bouscary and King, 2024), and (b) as a first-order system with activation energy of E_{eff}=0.92 eV and thermal escape frequency s_{th}=55 s^{-1} (cf. Guralnik and Sohbati, 2019). Such thermal stability parameters are obviously a generous approximation, given that significant differences in sample-specific E and s_{th} have been documented (Guralnik et al., 2015), and given that the mentioned E_{eff} and s_{th} are only "apparent" values, averaging over several kinetic processes to and from the excited state of the IRSL electron trap (cf. Guralnik and Sohbati, 2019). Nevertheless, the novelty of Eq. (22) is that it is the first explicit and to-date the most compact model, that can quantitatively predict the observed $IRSL_{50}$ data at 12 different depths of the KTB site (Appendix D) with a minimum of parameters and input data (Appendix C). The latter is achieved via convolution of two equilibrium factors, one thermal (θ) and one athermal (f), which appears powerful in replacing extensive Monte-Carlo simulations (Guralnik et al., 2015) with a single and straightforward one-line expression (Eq. 22).

5. Discussion and conclusions

The primary aim of the present contribution is the disentanglement of the mathematical treatment of anomalous fading, where historical inaccuracies have resulted in rather convoluted calculation schemes, that even seasoned practitioners have a hard time navigating. Our paper demonstrates that the two most popular fading corrections (Huntley and Lamothe, 2001; Kars et al., 2008) are amenable to a closed-form explicit solutions, which reduce practitioner dependence on computational brute force, and provide mathematical clarity and intuition regarding sensitivity of the fading correction to the various model parameters involved. The validity of our mathematics has been demonstrated via comparison of our new equations vis-à-vis legacy Monte-Carlo approaches in two classic archives, one from a sedimentary sequence (Section 4) and another from a thermochronological context (Section 5).

While this paper is not aimed at answering the commonly posed question regarding "which model is right", our present exercise does allow us to make cautious remarks about model validity and applicability. Here, it appears that ages corrected using the Huntley and Lamothe (2001) scheme are systematically younger than those obtained by the Kars et al. (2008) correction, and although this is not a new observation, our analysis highlights that this offset has little to do with linearity of signal growth, but rather stems from (a) the unphysical nature of logarithmic loss (Eq. 4), and (b) reflects an arbitrary offset arising from the "–1" term in Eq. (9). These effects (a and b) diminish as soon as the Huntley and Lamothe (2001) core scheme is upgraded to a power-law decay (Eq. 18), which is an overlooked yet necessary outcome of Visocekas' (1976, 1985) own quantification of anomalous fading.

Unlike the empirical/heuristic expressions for logarithmic (Eq. 4) or "power law" (Eq. 5) decays, nearest-neighbor distribution decay (Eq. 7) is a physically-driven model, traceable to the now seemingly forgotten research on electron traps in ZnS phosphors (Hoogenstraaten, 1958). In the limited example considered in Section 4, we demonstrated that all age corrections utilizing NND decay yielded age estimates consistent with the "conventional" independent age of the sedimentary unit in question. It is important to note, that NND-based models resulted in a cluster of corrected ages, regardless of whether charge retrapping is only implicit (Eq. 18), or whether NND decay was coupled to first-order (Eqs. 13/16-17) or higher-order (Eqs. 20-21)

https://doi.org/10.5194/egusphere-2025-4186
Preprint. Discussion started: 11 September 2025

charge retrapping models. The main takeaway from this exercise is that the choice of the particular retrapping model, as methodologically important as it might be, seems to exert only a second-order effect on the fading correction, while NND is the only truly physics-based "anomalous fading" model whose results are in line with independent age control.

From Figs. 4a-b, it is evident that standard laboratory experiments (including the dose response and the isothermal decay of the total target IRSL signal) appear insufficient for confirming or disproving the validity of the various decay and accumulation models discussed – as all the latter fit the available laboratory data equally well. The good news is that luminescence age correction seems to be overall resilient to varying formulations of the trapping-detrapping system (cf. King et al., 2018). The more challenging news is that in order to further increase the accuracy of fading-corrected IRSL ages via a better informed model choice, one will have to either conduct studies in archives where impeccable datasets of independent ages are available (cf. Section 4.4 for a cautionary tale), or that a more rigorous laboratory characterization of IRSL signal sub-components will become necessary to both justify and elucidate the parameters of the nonlinear signal growth models (e.g. Eqs. 20-21).

As a final remark, it appears that Eq. (18) is a plausible replacement for the legacy Huntley and Lamothe (2001) age correction, whenever no information on dose response is available, while variants of the Kars et al. (2008) model (Eqs. 13, 16-17, 20-21) can be utilized whenever the luminescence system is suspected to deviate from linear accumulation, en route to signal saturation (or more broadly, field steady-state).

6. Supplementary information

For full transparency and reproducibility of our mathematical results and all numerical exercises, commented Matlab scripts reproducing all tabulated and plotted results are provided as an online-only supplement.

7. Author contributions

BG conceived the study and developed the analytical expressions. GK and BG contributed to validation of the models and writing of the manuscript.

8. References

Aitken, M. J.: Thermoluminescence Dating. Academic Press, Orlando/London, 351 pp., 1985.

Auclair, M., Lamothe, M. and Huot, S.: Measurement of anomalous fading for feldspar IRSL using SAR. Radiat. Meas. 37, 487-492, https://doi.org/10.1016/S1350-4487(03)00018-0, 2003.

Beck, J.V.: Sensitivity coefficients utilized in nonlinear estimation with small parameters in a heat transfer problem. J. Basic Eng. 92, 215-221, https://doi.org/10.1115/1.3424973, 1970.

Bouscary, C., and King, G.E. Exploring the use of averaged thermal kinetic parameters in luminescence thermochronology. Radiat. Meas., 107215, https://doi.org/10.1016/j.radmeas.2024.107215, 2024.

Corless, R.M., Gonnet, G.H., Hare, D.E., Jeffrey, D.J. and Knuth, D.E.: On the Lambert W function. Adv. Comput. Math. 5, 329-359. https://doi.org/10.1007/BF02124750, 1996.

Guralnik, B., and Sohbati, R.: Fundamentals of luminescence photo-and thermochronometry. In Advances in physics and applications of optically and thermally stimulated luminescence, 399-437. https://doi.org/10.1142/9781786345790_0011, 2019.

Guralnik, B., Jain, M., Herman, F., Ankjærgaard, C., Murray, A.S., Valla, P.G., Preusser, F., King, G.E., Chen, R., Lowick, S.E., and Kook, M.: OSL-thermochronometry of feldspar from the KTB borehole, Germany. Earth Planet. Sci. Lett., 423, 232-243, https://doi.org/10.1016/j.epsl.2015.04.032, 2015.

Guralnik, B., Matmon, A., Avni, Y., Porat, N. and Fink, D., Constraining the evolution of river terraces with integrated OSL and cosmogenic nuclide data. Quat. Geochron., 6, 22-32, https://doi.org/10.1016/j.quageo.2010.06.002, 2011.

Hoogensraaten, W.: Electron traps in ZnS phosphors. Philips Res. Rep. 13, 515-693. 1958.

Huntley, D. J.: An explanation of the power-law decay of luminescence. J. Phys. Condens. Matter, 18, 1359, https://doi.org/10.1088/0953-8984/18/4/020, 2006.

Huntley, D.J., and Lamothe, M.: Ubiquity of anomalous fading in K-feldspars and the measurement and correction for it in optical dating. Can. J. Earth Sci. 38, 1093-1106, https://doi.org/10.1139/e01-013, 2001.

https://doi.org/10.5194/egusphere-2025-4186
Preprint. Discussion started: 11 September 2025

Ito, H.: Simultaneous U–Pb and U–Th dating using LA-ICP-MS for young (< 0.4 Ma) minerals: A reappraisal of the double dating approach. Minerals, 14, 436, https://doi.org/10.3390/min14040436, 2024.

Jaiswal, M.K., Bhat, M.I., Bali, B.S., Ahmad, S., and Chen, Y.G.: Luminescence characteristics of quartz and feldspar from tectonically uplifted terraces in Kashmir Basin, Jammu and Kashmir, India. Radiat. Meas., 44, 523-528, https://doi.org/10.1016/j.radmeas.2009.04.008, 2009.

Kars, R.H., Wallinga, J., and Cohen, K.M.: A new approach towards anomalous fading correction for feldspar IRSL dating—tests on samples in field saturation. Radiat. Meas., 43, 786-790, https://doi.org/10.1016/j.radmeas.2008.01.021, 2008.

King, G.E., Burow, C., Roberts, H.M., and Pearce, N.J.: Age determination using feldspar: evaluating fading-correction model performance. Radiat. Meas., 119, 58-73, https://doi.org/10.1016/j.radmeas.2018.07.013, 2018.

King, G.E., Herman, F., Lambert, R., Valla, P.G., and Guralnik, B.: Multi-OSL-thermochronometry of feldspar. Quat. Geochron., 33, 76-87, https://doi.org/10.1016/j.quageo.2016.01.004, 2016.

Lamothe, M., Auclair, M., Hamzaoui, C., and Huot, S.: Towards a prediction of long-term anomalous fading of feldspar IRSL. Radiat. Meas., 37, 493-498, https://doi.org/10.1016/S1350-4487(03)00016-7, 2003.

Lóczi, L., Guaranteed-and high-precision evaluation of the Lambert W function. Appl. Math. Comp. 433, 127406, https://doi.org/10.1016/j.amc.2022.127406, 2022.

Matsumoto, A. K-Ar age determination for Quaternary volcanic rocks based on the Mass Fractionation Correction Method – methodology and its application to Ontake and Aso volcanoes, Ph. D. Thesis, 153 pp., Univ. Tokyo, Japan, https://doi.org/10.11501/3087347, 1990.

Pagonis, V., Kitis, G. and Chen, R., A new analytical equation for the dose response of dosimetric materials, based on the Lambert W function. J. Lumin. 225, 117333, https://doi.org/10.1016/j.jlumin.2020.117333, 2020.

Renne, P.R., Progress and challenges in K-Ar and 40Ar/39Ar geochronology, Paleontol. Soc. P. 12, 47-66, https://doi.org/10.1017/S1089332600001340, 2006.

Rutherford, E.: XI. Radioactivity produced in substances by the action of thorium compounds. Phil. Mag. 49, 1-14, https://doi.org/10.1080/14786440009463832, 1900.

Slater, C., Preston, T., and Weaver, L. T.: Stable isotopes and the international system of units. Rapid Commun. Mass. Spectrom., 15, 1270-1273. https://doi.org/10.1002/rcm.328, 2001.

Smertenko, P.S.: Modeling of thermometric characteristics of thermodiode sensors by using the dimensionless sensitivity. Semicond. Phys. Quantum Electron. Optoelectron. 23, 437-441, https://doi.org/10.15407/spqeo23.04.437, 2020.

Smith, D.L.: Concept and significance of a dimensionless sensitivity matrix in applications of generalized least-squares analysis. Nucl. Instr. Methods A 339, 626-629, https://doi.org/10.1016/0168-9002(94)90203-8, 1994.

Tachiya, M., and Mozumder, A.: Decay of trapped electrons by tunnelling to scavenger molecules in low-temperature glasses. Chem. Phys. Lett. 28, 87-89, https://doi.org/10.1016/0009-2614(74)80022-9, 1974.

Thiel, C., Tsukamoto, S., Tokuyasu, K., Buylaert, J.P., Murray, A.S., Tanaka, K. and Shirai, M.: Testing the application of quartz and feldspar luminescence dating to MIS 5 Japanese marine deposits. Quat. Geochron., 29, 16-29, https://doi.org/10.1016/j.quageo.2015.05.008, 2015.

Thomas, D.G., Hopfield, J.J. and Augustyniak, W.M., Kinetics of radiative recombination at randomly distributed donors and acceptors. Phys. Rev. 140, A202, https://doi.org/10.1103/PhysRev.140.A202, 1965.

Visocekas, R. Miscellaneous aspects of artificial thermoluminescence of calcite: Emission spectra, athermal detrapping and anomalous fading. Eur. PACT J. 3, 258-265, 1976.

Visocekas, R.: Tunnelling radiative recombination in labradorite: its association with anomalous fading of thermoluminescence. Nucl. Tracks Radiat. Meas., 10, 521-529, https://doi.org/10.1016/0735-245X(85)90053-5, 1985.

Visocekas, R.: Tunnelling radiative recombination in labradorite: its association with anomalous fading of thermoluminescence. Nucl. Tracks Radiat. Meas., 10, 521-529, https://doi.org/10.1016/0735-245X(85)90053-5, 1985.

Wintle, A. G.: Anomalous fading of thermo-luminescence in mineral samples. Nature, 245, 143-144, https://doi.org/10.1038/245143a0, 1973.

https://doi.org/10.5194/egusphere-2025-4186
Preprint. Discussion started: 11 September 2025

Appendix A: Data for samples from Oga peninsula (MIS 5 Japanese marine deposits).

Sample ID	$\dot{D}_{nat}$ (Gy/ka)	D_e (Gy)	g_{2d} (%/decade)	Corrected age * (ka)
055257	1.77 ± 0.14	132 ± 8	2.0 ± 0.1	91 ± 6
055256	1.58 ± 0.13	121 ± 11	1.9 ± 0.1	92 ± 8
055255	1.64 ± 0.14	121 ± 8	2.2 ± 0.1	92 ± 6
055254	1.99 ± 0.15	138 ± 10	1.7 ± 0.2	82 ± 6
055253	1.90 ± 0.15	138 ± 9	1.9 ± 0.1	87 ± 6
055252	2.00 ± 0.15	138 ± 12	2.3 ± 0.2	87 ± 8
055251	1.78 ± 0.14	131 ± 9	2.2 ± 0.1	92 ± 6
055250	1.84 ± 0.15	132 ± 8	1.8 ± 0.1	85 ± 5
055249	1.73 ± 0.14	136 ± 10	2.1 ± 0.1	97 ± 7
055248	2.10 ± 0.16	137 ± 7	2.0 ± 0.1	80 ± 4
055247	2.04 ± 0.16	142 ± 10	1.8 ± 0.1	83 ± 6
055246	1.94 ± 0.15	154 ± 9	1.3 ± 0.6	90 ± 8
055245	1.95 ± 0.14	142 ± 9	2.3 ± 0.2	92 ± 6
055244	2.00 ± 0.15	141 ± 9	1.8 ± 0.2	84 ± 5
055242	1.97 ± 0.15	137 ± 7	2.1 ± 0.2	86 ± 5
055243	1.88 ± 0.14	151 ± 8	1.7 ± 0.1	94 ± 5
055241	1.97 ± 0.15	150 ± 10	2.0 ± 0.2	93 ± 7
055240	1.98 ± 0.15	136 ± 9	2.0 ± 0.1	84 ± 5
055239	1.88 ± 0.14	166 ± 8	2.0 ± 0.2	108 ± 6
055237	1.93 ± 0.14	155 ± 10	2.3 ± 0.2	102 ± 7
055231	1.78 ± 0.14	152 ± 11	1.4 ± 0.6	98 ± 12
055232	1.66 ± 0.14	167 ± 12	2.3 ± 0.1	128 ± 14
055233	1.75 ± 0.14	217 ± 10	1.5 ± 0.1	144 ± 13
055234	1.95 ± 0.14	215 ± 9	2.1 ± 0.1	136 ± 12
055236	1.85 ± 0.13	258 ± 16	1.9 ± 0.1	170 ± 16

Feldspar post-IR IR_{225} measurements for the sedimentary samples from Thiel et al. (2015).
* As published (reported using the Huntley and Lamothe, 2001 correction).

https://doi.org/10.5194/egusphere-2025-4186
Preprint. Discussion started: 11 September 2025

Appendix B: Simulated ages and uncertainties for Oga peninsula (all in units of ka).

Model	Huntley and Lamothe (2001)				Kars et al. (2008)			
Solution*	SA	MC	A		SA	MC	A	
ID \ Eq.	9		10	11	13		16	17
055257	90.237	90.861 ± 9.243	90.237 ± 9.038		98.060	98.625 ± 10.337	98.553 ± 9.923	
055256	91.820	92.308 ± 11.507	91.820 ± 11.297		98.977	100.137 ± 12.516	99.523 ± 12.285	
055255	91.178	91.756 ± 10.115	91.178 ± 9.890		99.409	100.181 ± 11.540	99.959 ± 10.888	
055254	81.344	81.836 ± 8.858	81.344 ± 8.656		87.391	87.967 ± 9.933	87.838 ± 9.519	
055253	86.948	87.530 ± 9.171	86.948 ± 8.946		94.224	95.314 ± 10.167	94.735 ± 9.798	
055252	85.980	86.371 ± 10.265	85.980 ± 10.031		94.750	95.644 ± 12.262	95.233 ± 11.280	
055251	90.881	91.548 ± 9.708	90.881 ± 9.537		99.476	100.741 ± 11.128	100.024 ± 10.547	
055250	85.044	85.489 ± 8.863	85.044 ± 8.681		91.622	92.557 ± 9.645	92.080 ± 9.446	
055249	96.124	96.660 ± 10.912	96.124 ± 10.556		105.051	105.286 ± 12.318	105.626 ± 11.653	
055248	78.807	79.326 ± 7.585	78.807 ± 7.273		85.685	86.102 ± 8.421	86.122 ± 7.998	
055247	82.449	83.082 ± 8.941	82.449 ± 8.729		89.083	89.572 ± 9.851	89.530 ± 9.526	
055246	89.573	90.338 ± 10.313	89.573 ± 10.115		95.041	96.379 ± 12.790	95.457 ± 12.412	
055245	90.774	91.041 ± 9.074	90.774 ± 8.893		100.256	101.263 ± 10.757	100.769 ± 10.093	
055244	83.520	83.989 ± 8.442	83.520 ± 8.392		90.221	90.511 ± 9.774	90.674 ± 9.302	
055242	84.916	85.498 ± 8.111	84.916 ± 7.975		92.743	93.272 ± 9.106	93.242 ± 8.962	
055243	94.271	94.709 ± 8.833	94.271 ± 8.666		101.775	102.656 ± 10.068	102.307 ± 9.471	
055241	92.053	92.510 ± 9.737	92.053 ± 9.500		100.704	101.089 ± 11.471	101.208 ± 10.667	
055240	83.021	83.707 ± 8.642	83.021 ± 8.393		90.278	90.536 ± 9.568	90.736 ± 9.221	
055239	106.818	107.453 ± 10.054	106.818 ± 9.720		117.728	118.717 ± 11.325	118.309 ± 11.094	
055237	100.145	100.778 ± 10.153	100.145 ± 9.940		111.342	111.530 ± 12.091	111.912 ± 11.375	
055231	97.350	98.308 ± 11.992	97.350 ± 11.865		103.801	104.619 ± 15.225	104.242 ± 14.377	
055232	125.697	126.567 ± 14.482	125.697 ± 13.989		140.837	142.939 ± 17.270	141.576 ± 15.848	
055233	142.821	143.995 ± 13.633	142.821 ± 13.261		156.118	157.663 ± 14.992	156.952 ± 14.723	
055234	134.763	135.567 ± 11.547	134.763 ± 11.285		152.695	153.363 ± 13.646	153.560 ± 13.036	
055236	167.156	168.130 ± 16.310	167.156 ± 15.758		191.021	192.282 ± 20.588	192.035 ± 18.357	

* SA: semianalytical; MC: Monte-Carlo simulation (N=1000); A: Analytical.

https://doi.org/10.5194/egusphere-2025-4186
Preprint. Discussion started: 11 September 2025

Appendix C: Data for samples from the KTB borehole.

Sample ID	Depth, z (km)	$\dot{D}_{nat}$ * (Gy/ka)	D_e † (Gy)		g_{2d} ◊ (%/decade)	D_0 ‡ (Gy)	$\dot{D}_{lab}$ § (Gy/s)
19B	0.146	1.50	275.2	35.2	1.845	171	0.18
48B	0.334	1.03	302.5	82.5	0.004	82	0.18
105B	0.566	2.92	365.2	56.2	1.107	179	0.18
146A	0.726	2.84	201.1	17.9	4.036	259	0.18
218A	0.911	2.96	239.6	20.8	3.089	241	0.18
253F	1.175	1.58	128.0	12.7	3.921	235	0.18
273G	1.300	1.07	96.1	13.3	4.230	201	0.18
314B	1.499	1.07	62.8	11.2	6.271	298	0.27
383C	1.730	3.02	89.3	18.9	1.987	200	0.25
428B	1.892	3.44	93.5	7.4	2.045	225	0.18
481B	2.097	3.57	56.9	11.9	2.216	229	0.25
564A	2.329	3.30	32.9	2.9	2.564	236	0.18

Subsurface bedrock samples from Guralnik et al. (2015).
* assigned 15% relative uncertainty.
† recalculated from the original publication via $D_e = -D_0 \ln(1 - L_{nat}/L_{labmax})$.
◊ recalculated using Eq. (5a) from sample-dependent ρ' and s values, and assigned 15% relative uncertainty.
‡ assigned 3% relative uncertainty.
§ the maximum laboratory dose rate (no uncertainties considered).

Appendix D: Simulated values for the KTB borehole.

Sample	Calculated parameters			Apparent ages in ka		
ID	θ	$f_{H\&L}$	f_{Kars}	Uncorrected	Eqs. 22&23	Eqs. 22&24
19B	1.01	0.84 ± 0.03	0.80 ± 0.03	183.5 ± 36.2	209.6 ± 38.1	185.3 ± 32.4
48B	1.00	N/A*	1.00 ± 0.00	293.7 ± 91.4	N/A*	458.8 ± 70.2
105B	0.99	0.90 ± 0.02	0.88 ± 0.02	125.1 ± 26.9	135.5 ± 22.5	123.1 ± 20.3
146A	0.96	0.66 ± 0.07	0.62 ± 0.04	70.8 ± 12.4	92.0 ± 22.1	81.7 ± 15.7
218A	0.92	0.74 ± 0.05	0.69 ± 0.04	81.0 ± 14.0	93.4 ± 18.6	83.3 ± 15.0
253F	0.73	0.67 ± 0.07	0.62 ± 0.04	81.0 ± 14.6	99.5 ± 21.3	89.4 ± 16.3
273G	0.60	0.64 ± 0.08	0.59 ± 0.05	89.8 ± 18.3	89.7 ± 19.8	81.1 ± 14.8
314B	0.36	0.48 ± 0.14	0.45 ± 0.05	58.7 ± 13.7	52.5 ± 19.2	48.5 ± 9.8
383C	0.54	0.83 ± 0.03	0.79 ± 0.03	29.6 ± 7.7	39.6 ± 6.4	37.1 ± 5.9
428B	0.44	0.83 ± 0.03	0.79 ± 0.03	27.2 ± 4.6	29.3 ± 4.7	27.6 ± 4.4
481B	0.32	0.81 ± 0.03	0.77 ± 0.03	15.9 ± 4.1	19.0 ± 3.0	17.9 ± 2.9
564A	0.19	0.79 ± 0.04	0.74 ± 0.03	10.0 ± 1.7	11.4 ± 1.8	10.7 ± 1.7

* results in numerical overflow of the Lambert W expression, signifying that the Huntley & Lamothe (2001) correction is degenerate due to a negligible fading rate.